PHYSICAL REVIEW E **90**, 051101(R) (2014)

# Mechanism of formation of subnanosecond current front in high-voltage pulse open discharge

I. V. Schweigert,[1,2] A. L. Alexandrov,[1] Dm. E. Zakrevsky,[3] and P. A. Bokhan[3]
[1]*Khristianovich Institute of Theoretical and Applied Mechanics, Novosibirsk 630090, Russia*
[2]*Novosibirsk State University, Novosibirsk 630090, Russia*
[3]*Rzhanov Institute of Semiconductor Physics, Novosibirsk 630090, Russia*
(Received 17 July 2014; published 3 November 2014)

The mechanism of subnanosecond current front rise observed previously in the experiment in high-voltage pulse open discharge in helium is studied in kinetic particle-in-cell simulations. The Boltzmann equations for electrons, ions, and fast atoms are solved self-consistently with the Poisson equations for the electrical potential. The partial contributions to the secondary electron emission from the ions, fast atoms, photons, and electrons, bombarding the electrode, are calculated. In simulations, as in the experiment, the discharge glows between two symmetrical cathodes and the anode grid in the midplane at $P = 6$ Torr and the applied voltage of 20 kV. The electron avalanche development is considered for two experimental situations during the last stage of breakdown: (i) with constant voltage and (ii) with decreasing voltage. For case (i), the subnanosecond current front rise is set by photons from the collisional excitation transfer reactions. For the case (ii), the energetic electrons swamp the cathode during voltage drop and provide the secondary electron emission for the subnanosecond current rise, observed in the experiment.

DOI: 10.1103/PhysRevE.90.051101 PACS number(s): 52.80.Tn, 52.65.Rr

The mechanism of development of breakdown in gas is the fundamental problem of the gas discharge physics, attracting considerable attention for the last decade (see, for example, [1,2]). Nevertheless, some new experimental observations could not be described in the framework of existing physical models and give us new material for discussion. For example, the current amplitude of 28 kA with the current front rise of 500 A/cm$^2$ ns was measured in Ref. [3] in a high-voltage pulse open (HVPO) discharge. So fast subnanosecond current front rise is a unique property of the HVPO discharge and the mechanism of its ignition is unknown. The discharge with such characteristics can be used for generation of high-energy electron beams or as a new subnanosecond electrical switch, triggering the voltage of a few tens of kilovolts.

In this work, in particle-in-cell (PIC) simulations, we study the mechanism governing the subnanosecond breakdown in HVPO discharge for the conditions of the experiment [3]. Recently, the breakdown development at times of tens of nanoseconds is investigated in PIC simulations in various gases and a wide pressure range (see, for example, [4–7]). In these works, the physical approach is restricted to electron and ion kinetics only and electron avalanche is created due to electron impact ionization. The inclusion of ion impact ionization and the secondary electron emission (SEE) by ions from a cathode surface in the physical model of He breakdown was made, for example, in [8], in order to simulate the particular shape of the Paschen curve. As a next step in the understanding of a breakdown mechanism in He, the fast atoms were included in the PIC model in [1]. The authors concluded that the fast atoms play a key role in discharge development due to their essential contribution to the SEE. The roles of different elementary processes with ions and fast atoms in the shape of the Paschen curve were analyzed. The PIC simulations of stationary high-voltage (HV) discharge in He [9] also confirmed that fast atoms make an important contribution to SEE. Similar conclusions were made in Ref. [2], using an analytical model.

Previously photoemission was not considered as a possible candidate for the breakdown in dc discharge. The photoemission coefficient, measured in clean vacuum conditions [10], was very small, $\gamma_{ph} \approx 0.03$–$0.05$. Nevertheless, it is known [10,11] that in HV discharges, the surfaces treated by energetic heavy particles are contaminated. Under these conditions the $\gamma_{ph}$ can be an order of magnitude larger than that in vacuum. The SEE coefficients for photons, ions, and fast atoms were revised in Refs. [12,13] in HV discharge experiments. The value of $\gamma_{ph} = 0.3$ was found for the resonant line of He (58.4 nm). For fast atoms, the SEE had a lower energy threshold of kinetic emission due to the atom absorption and implantation.

In this work, we developed the following model for kinetic simulation of the HVPO discharge in helium. The system of equations includes the Boltzmann equations for electrons, ions, fast atom distribution functions, and the Poisson equation for the electrical potential. All equations are solved self-consistently. The collisional integral in the right part of the Boltzmann equations includes elastic and inelastic collisions of colliding particles with background atoms. For electrons the angle of scattering and energies after ionization collision depends on the energy of colliding electrons [14]. For the electrons, three types of collisions are considered: (a) elastic, or momentum transfer [15], (b) excitation [16], and (c) ionization [16]. For $He^+$ ions, four types of collisions are taken into account: (a) isotropic and (b) backward elastic scattering [17], (c) excitation [18], and (d) ionization [19]. For the fast atoms $He_f$ four types of collisions are included: (a) elastic scattering [20], (b) excitation [21], (c) ionization [22], and (d) collisional excitation transfer (CET), $He_f + He^* = He_f^* + He$, where $He^*$ is an atom excited by electron impact. The cross sections for heavy species are shown in Fig. 1. The cross section of CET from ground to resonant state ($^1S$-$^1P$) is $\sigma_r = 2.25\pi e^2\mu^2/\hbar v$ [23], where $v$ is the relative velocity of colliding atoms and $\mu$ is the transition dipole matrix element between the $S$ and $P$ states. In helium, the $1^1S$-$2^1P$ CET reaction has $\sigma_r = 4.6 \times 10^{-14}/\sqrt{\varepsilon_a}$, cm$^2$ [24], where $\varepsilon_a$ is the fast atom

 

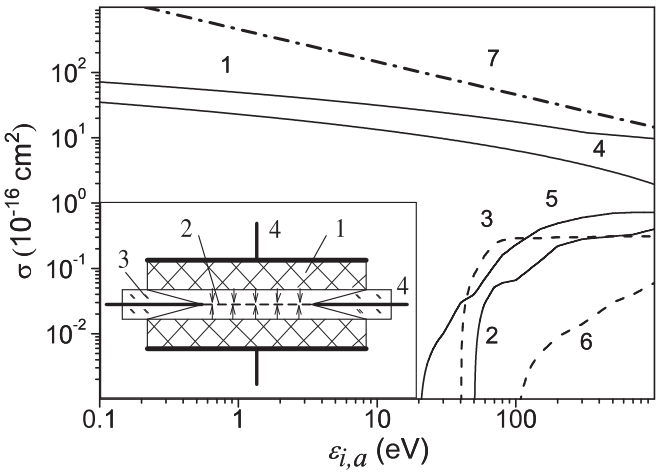


FIG. 1. Cross sections for $He^+$ ions and $He_f$ fast atoms in helium as a function of the energy of colliding particles. For ions: isotropic and backward elastic scattering (1), excitation (2), ionization (3). For fast atoms: elastic (4), excitation (5), ionization (6), CET (7). Inset shows the sketch of the experimental setup, cathode (1), anode grid (2), separating dielectric plates (3), and lead-in (4).

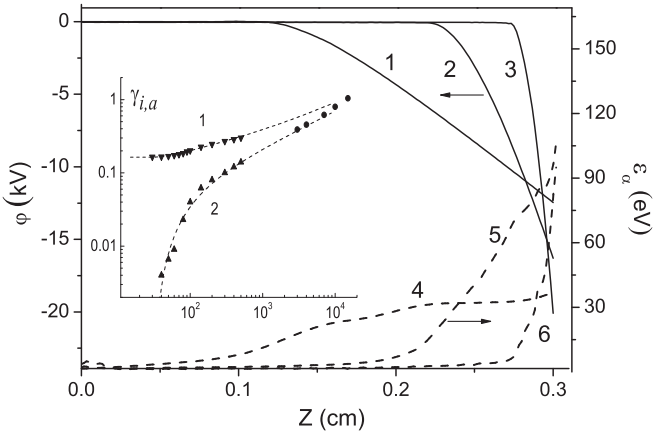


FIG. 2. Potential profiles (1,2,3) and fast atom energy distributions (4,5,6) for different times, $t = 44$ ns (1,4), 52 ns (2,5), and 60 ns (3,6) for $P = 6$ Torr. Inset shows the electron emission yield $\gamma_i$ for ions (1) and $\gamma_a$ for fast atoms (2) from experiments [12] (triangles, in HV discharge) and [25] (circles, in vacuum).

energy in eV. The fast atoms $He_f$ appear due to scattering of ions on background atoms. We include into consideration only the fast atoms with the energy $\varepsilon_a > 1$ eV.

In our model, the ions, fast atoms, and electrons (with the energy $\varepsilon_e > \varepsilon_0$), crossing the anode grid, are lost with the probability of 0.02, since the transparency of the grid in the experiment is 98%. The anode grid is supposed to be negatively charged and the electrons with the energy $\varepsilon_e < \varepsilon_0$ are reflected from the grid. In simulations, the value of $\varepsilon_0$ ranged from 100 to 300 eV and we did not find a visible difference in electron avalanche development for various $\varepsilon_0$.

We assume that only the photons with a Doppler shift (DS) can reach the cathode surface during breakdown and provide the photoemission. The Doppler shift of radiated photons is provided by the momentum transfer during reaction between heavy particles. In our simulation, the Doppler shifted photons appear due to three reactions: excitation of background atoms (1) by ions, (2) by fast neutrals, and (3) in the collisional excitation transfer between excited atoms and fast neutrals. In our model, the DS photons instantly reach the cathode after the excitation since they propagate in plasma as in vacuum without reabsorption. In contrast, the photons, radiated after the excitation by electron impact, are trapped in the plasma due to the multiple reabsorption and do not reach the cathode during breakdown.

In simulations as in the experiment [3], the discharge glows in a narrow gap ($d = 0.6$ cm) between two cathodes and a grid anode in the midplane (see inset in Fig. 1). The cathode area is large, 16.8 cm × 3 cm, and it allows us to use a one-dimensional model. The gas pressure is $P = 6$ or 15 Torr. The voltage on the cathode, $U(t) = U_0 \sin(\pi/4 \times t/t^*)$, first increases during $t < t^* = 60$ ns up to the maximum value of −20 kV (or −13 kV). Then at $t > t^*$ two different experimental situations can take place. We consider case (i), when the voltage remains constant during breakdown, $U(t) = U_0$, and case (ii), when the voltage changes from the maximum to −100 V during 0.5 ns during breakdown. In simulations we take the coefficients $\gamma_i$ and $\gamma_a$ [12] shown in the inset in Fig. 2, $\gamma_{ph} = 0.3$ and $\gamma_e = 0.5$ (SEE by electrons). The simulation grid is uniform with $\Delta x = 0.001$ cm, which is less than the Debye length. The time step is $\Delta t = 5 \times 10^{-16}$ s. It is restricted by the Courant number ($\Delta x/v_e = 10^{-12}$ s) and the plasma frequency ($\omega_e = 10^{12}$ s$^{-1}$). The number of pseudoparticles for every species is $1.5 \times 10^4$ in the beginning of simulation. Then during the electron avalanche development the initial weight of pseudoparticles is recalculated to avoid the exponential growth of the number of pseudoparticles. At the final stage of calculation the number of pseudoparticles increases up to $10^6$.

We start simulation with the plasma density equal to $n_e = n_i = 10^5$ cm$^{-3}$. At the beginning the electrical potential has a linear distribution between the anode and cathode. With the growth of the plasma density, the quasineutral area first appears in the center of discharge and then extends to the cathode direction. In Fig. 2, the electrical potential profiles and the fast atom energy distribution are shown for different times. As seen from the potential profiles, the sheath forms near the cathode (placed at $Z = 0.3$ cm). The electrons emitted from the cathode gain the energy, crossing the cathode sheath, where the electrical field strength is large. Since the anode grid is practically transparent, the electrons oscillate between two cathodes providing a high ionization rate.

*Case (i).* First, let us consider the evolution of current when the voltage remains constant during the breakdown, i.e., $U(t) = U_0$ for $t > t^*$. In Fig. 3(a), the ion $n_i$ and fast atom $n_a$ density profiles are shown for various stages of ignition. Since the ion free path is $l_{ex} \approx 0.0025$ cm, an ion can produce 10–40 fast atoms within the cathode sheath. Therefore the density of fast atoms is larger than that for ions [see Fig. 3(a)]. In the bulk plasma, the electron density $n_e \approx n_i$, but within the sheath $n_e \ll n_i$, since the density of the emitted electrons from the cathode surface is small. The density of atoms $He^*$ excited by electron impact is about 20% higher than the plasma density. In Fig. 3(b), the excitation rates by ions, fast atoms, and in

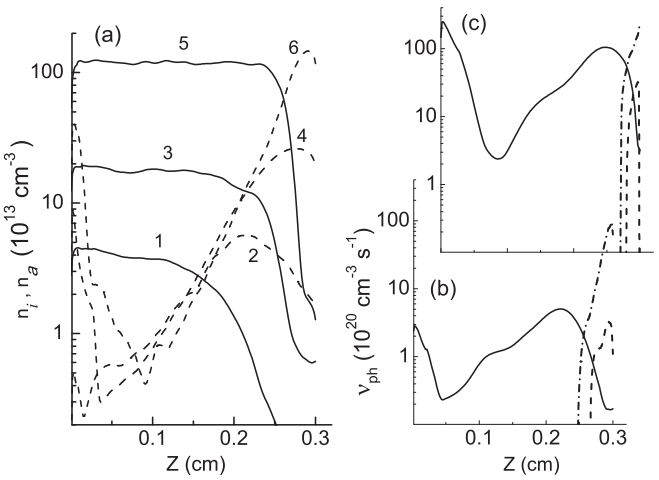


FIG. 3. (a) Ion and fast atom density distributions for different times, $t = 52$ ns, $n_i$ (1) and $n_a$ (2), $t = 56$ ns, $n_i$ (3) and $n_a$ (4), $t = 60$ ns, $n_i$ (5) and $n_a$ (6). (b), (c) Volume production rate of DS photons $\nu_{ph}$, by ions (dashed curves), fast atoms (dash-dotted curves), and in collisional excitation transfer reactions (solid curves), at $t = 56$ ns (b) and 60 ns (c).

CET reactions are shown for two times. For $t = 56$ ns the DS photon productions from different channels are comparable, but for $t = 60$ ns the CET reaction ($He_f + He^* = He^*_f + He$) dominates.

We have found three stages of the breakdown. In Fig. 4(a), the SEE currents from the cathode due to the bombardment by DS photons $j^e_{ph}$, ions $j^e_i$, and fast atoms $j^e_a$ are shown. The contribution from the electron bombardment is negligible for case (i). In the first stage of breakdown, at $t < t_1$, the SEE is set by the DS photons. These DS photons appear due to the excitation of background gas by fast atoms and ions within the cathode sheath, where the energy of heavy particles is large (see Fig. 2). Note that the excitation rate by ions is much less

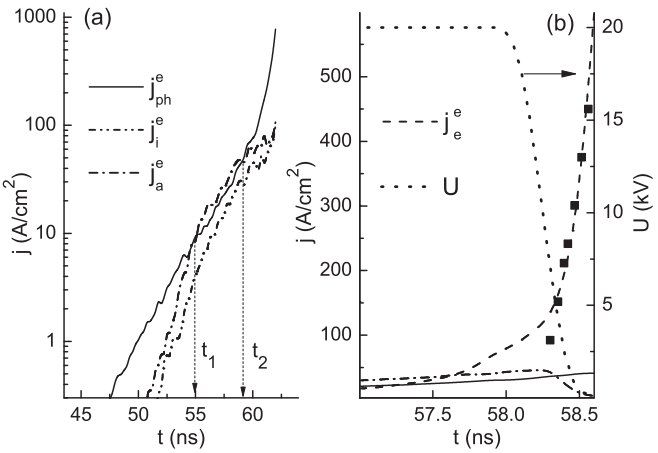


FIG. 4. Secondary electron emission currents from cathode due to the bombardment by photons (solid curve), ions (dash-dot-dotted curve), fast atoms (dash-dotted curve), and electrons (dashed curve) vs time for case (i) (a) and for case (ii) (b). Symbols are the total current from [3]. The arrows point out the different stages of breakdown.

than by fast atoms. The general role of ions is the production of fast atoms. In the second stage of breakdown, at $t_1 < t < t_2$, $j^e_{ph} \approx j^e_n \approx 2 \times j^e_i$. In the third stage, at $t > t_2$, the SEE current is again determined by the flux of DS photons to the cathode surface, but these photons appear from another type of reaction when compared to the first stage. The accumulation of the excited atoms $He^*$ and the fast atoms $He_f$ in the discharge volume leads to an increase of the rate of CET reaction, $He_f + He^* = He^*_f + He$. It becomes the most important source of the DS photons, which can reach the cathode without reabsorption.

The density of excited atoms $He^*$ rises with time because of the high electron excitation rate, low diffusion losses, and multiple reabsorption of photons radiated by excited atoms $He^*$. The characteristic times of losses of $He^*$ due to diffusion on the electrodes and the photon transport to the cathode are much greater than the breakdown time. The production of DS photons by fast atoms becomes smaller during breakdown. The energy of fast atoms exceeds the excitation threshold only in the cathode sheath (see Fig. 2), which becomes narrower with an increase of the plasma density.

We have performed additional calculations of the breakdown development without CET reaction to estimate its contribution in current development. We found that at this condition the current is not able to exhibit the growth rate of 500 A/cm$^2$ ns. We also analyzed the effect of the step ionization and the ionization from collisions of two excited atoms on the electron current evolution. Our calculation results showed that these processes made a weak contribution in the ionization rate for our parameters.

*Case (ii)*. Let us consider the SEE evolution during breakdown when the voltage drops. In Ref. [3], the voltage changes from −20 kV (or −13 kV) to −100 V during 0.5 ns when the current starts to grow. In case (ii), the scenario of the third stage of development of electron avalanche is completely different from case (i). In Fig. 4(b), the evolution of SEE currents calculated and measured in [3] is shown. One can see that the SEE current from the electron bombardment dominates in the third stage of breakdown. With decreasing voltage, the high-energy electrons begin to swamp the cathode surface. The number of these electrons is large, since the frequency of electron inelastic collisions is $10^{10}$ s$^{-1}$, and the thermalization of the 20 kV electrons lasts about 100 ns. In this case the SEE by electrons determines the electron avalanche development [see Fig. 4(b)].

In conclusion, the mechanism of electron avalanche development in HVPO discharge in helium has been studied in kinetic PIC simulations for the conditions of the experiment [3]. The discharge glows between two symmetrical cathodes and the anode grid in the center at $P = 6$ Torr (or 15 Torr) and the applied voltage of 20 kV (or 13 kV). The ignition of HVPO discharge has been considered for two experimental situations when during breakdown the voltage is constant [case (i)] and changes from −20 kV (or −13 kV) to −100 V [case (ii)]. The partial contributions of fluxes of photons, ions, fast atoms, and electrons on the cathode to the SEE were calculated.

We have found three stages of the breakdown development. In the first stage, the SEE is provided by DS photons from the excitation of background atoms by fast atoms. In the second stage, these photons, fast atoms, and ion fluxes on

the cathode contribute equally to the SEE. In the third stage, the mechanism of electron avalanche is different for the experimental situations with the constant voltage and decreasing voltage. For case (i), the subnanosecond current front rise is set by CET reaction, $He_f + He^* = He^*_f + He$. For case (ii), the energetic electrons swamp the cathode during voltage decrease and provide enhanced SEE for the subnanosecond current rise, observed in the experiment [3]. Both in simulations and in experiments the gas pressure changed from 6 Torr to 15 Torr. With increasing $P$, the frequencies of collisions rose and the time interval $t_1$ became smaller [see Fig. 4(a)]. This is explained by more rapid accumulation of fast and excited atoms. The change of the voltage from 20 kV to 13 kV did not give a visible effect to the electron avalanche dynamics.

Note, that the large value of $\gamma_{ph} = 0.3$ measured for our discharge conditions in [12] is very important for the description of a subnanosecond breakdown scenario. The variation of $\gamma_i$ and $\gamma_a$ is not so critical, since they determine the current growth only at the second stage, $t_1 < t < t_2$. The value of the $\gamma_e$ is important only for case (ii) and $\gamma_e > 0.5$ provides the current growth rate observed in the experiment.

This work was supported by the Russian Foundation for Basic Research (RFBR), Grant No. 13-08-00375.

[1] P. Hartmann, Z. Donkó, G. Bánó, L. Szalai, and K. Rózsa, Plasma Sources Sci. Technol. **9**, 183 (2000).
[2] B. M. Jelenković and A. V. Phelps, Phys. Rev. E **71**, 016410 (2005).
[3] P. A. Bokhan, P. P. Gugin, Dm. E. Zakrevsky, and M. A. Lavrukhin, Tech. Phys. Lett. **39**, 775 (2013).
[4] E. Kh. Baksht, S. Ya. Belomyttsev, A. G. Burachenko, V. V. Ryzhov, V. F. Tarasenko, and V. A. Shklyaev, Tech. Phys. **57**, 998 (2012).
[5] C. G. Yang, L. Duan, Y. Y. Xu, X. B. Wang, and D. Zuo, Phys. Plasmas **19**, 093510 (2012).
[6] L. Pang, F. B. Tao, B. Z. Ren, and Q. G. Zhang, IEEE Trans. Plasma Sci. **40**, 919 (2010).
[7] J. Sun, C. Sang, T. Stirner, and D. Wang, J. Phys. D: Appl. Phys. **43**, 275201 (2010).
[8] H. Hillmann, F. Muller, and H. Wenz, Plasma Sources Sci. Technol. **3**, 496 (1994).
[9] P. Hartmann, H. Matsuo, Y. Ohtsuka, M. Fukao, M. Kando, and Z. Donkó, Jpn. J. Appl. Phys. **42**, 3633 (2003).
[10] A. V. Phelps and Z. Lj Petrovic, Plasma Sources Sci. Technol. **8**, R21 (1999).
[11] L. N. Dobretsov and M. V. Gomoyunova, *Emission Electronics* (Israel Program for Scientific Translations, Jerusalem, 1971).
[12] P. A. Bokhan and Dm. E. Zakrevsky, Tech. Phys. **52**, 104 (2007).
[13] P. A. Bokhan and Dm. E. Zakrevsky, Phys. Rev. E **88**, 013105 (2013).
[14] C. B. Opal, W. K. Peterson, and E. C. Beaty, J. Chem. Phys. **55**, 4100 (1971).
[15] L. L. Alves, K. Bartschat, S. F. Biagi *et al.*, J. Phys. D: Appl. Phys. **46**, 334002 (2013).
[16] Yu. Ralchenko, R. K. Janev, T. Kato, D. V. Fursa, I. Bray, and F. J. de Heer, At. Data Nucl. Data Tables **94**, 603 (2008).
[17] W. H. Cramer and J. H. Simons, J. Chem. Phys. **26**, 1272 (1957).
[18] R. Okasaka, Y. Konishi, Y. Sato, and K. Fukuda, J. Phys. B: At. Mol. Phys. **20**, 3771 (1987).
[19] H. B. Gilbody and J. B. Hasted, Proc. R. Soc. Lond. A **240**, 382 (1957).
[20] J. E. Jordan and I. Amdur, J. Chem. Phys. **46**, 165 (1967).
[21] V. Kempter, F. Veith, and L. Zehnle, J. Phys. B: At. Mol. Phys. **8**, 1041 (1975).
[22] H. C. Hayden and N. G. Utterback, Phys. Rev. **135**, A1575 (1964).
[23] I. I. Sobelman, L. A. Vainshtein, and E. A. Yukov, *Excitation of Atoms and Broadening of Spectral Line* (Springer-Verlag, Berlin, 1981).
[24] T. Watanabe, Phys. Rev. **138**, A1573 (1965).
[25] R. A. Baragiola, E. V. Alonso, and A. Oliva Florio, Phys. Rev. B **19**, 121 (1979).